DOI: 10.1111/jbi.13125

ORIGINAL ARTICLE

WILEY Journal of Biogeography

Demographic modelling reveals a history of divergence with gene flow for a glacially tied stonefly in a changing post-Pleistocene landscape

Scott Hotaling[1] | Clint C. Muhlfeld[2,3] | J. Joseph Giersch[2] | Omar A. Ali[4] | Steve Jordan[5] | Michael R. Miller[4] | Gordon Luikart[6] | David W. Weisrock[1]

[1]Department of Biology, University of Kentucky, Lexington, KY, USA

[2]U.S. Geological Survey, Northern Rocky Mountain Science Center, Glacier Field Station, Glacier National Park, West Glacier, MT, USA

[3]Flathead Lake Biological Station, The University of Montana, Polson, MT, USA

[4]Department of Animal Science, University of California, Davis, CA, USA

[5]Department of Biology, Bucknell University, Lewisburg, PA, USA

[6]Montana Conservation Genomics Laboratory, Division of Biological Sciences, Flathead Lake Biological Station, The University of Montana, Polson, MT, USA

Correspondence
Scott Hotaling, School of Biological Sciences, Washington State University, Pullman, WA, USA.
Email: scott.hotaling@wsu.edu

Present address
Scott Hotaling, School of Biological Sciences, Washington State University, Pullman, WA, USA.

Funding information
USGS Northern Rocky Mountain Science Center; Great Northern Landscape Conservation Cooperative; Glacier National Park Conservancy

Editor: Peter Pearman

Abstract

Aim: Climate warming is causing extensive loss of glaciers in mountainous regions, yet our understanding of how glacial recession influences evolutionary processes and genetic diversity is limited. Linking genetic structure with the influences shaping it can improve understanding of how species respond to environmental change. Here, we used genome-scale data and demographic modelling to resolve the evolutionary history of *Lednia tumana*, a rare, aquatic insect endemic to alpine streams. We also employed a range of widely used data filtering approaches to quantify how they influenced population structure results.

Location: Alpine streams in the Rocky Mountains of Glacier National Park, Montana, USA.

Taxon: *Lednia tumana*, a stonefly (Order Plecoptera) in the family Nemouridae.

Methods: We generated single nucleotide polymorphism data through restriction-site associated DNA sequencing to assess contemporary patterns of genetic structure for 11 *L. tumana* populations. Using identified clusters, we assessed demographic history through model selection and parameter estimation in a coalescent framework. During population structure analyses, we filtered our data to assess the influence of singletons, missing data and total number of markers on results.

Results: Contemporary patterns of population structure indicate that *L. tumana* exhibits a pattern of isolation-by-distance among populations within three genetic clusters that align with geography. Mean pairwise genetic differentiation (F_{ST}) among populations was 0.033. Coalescent-based demographic modelling supported divergence with gene flow among genetic clusters since the end of the Pleistocene (~13-17 kya), likely reflecting the south-to-north recession of ice sheets that accumulated during the Wisconsin glaciation.

Main conclusions: We identified a link between glacial retreat, evolutionary history and patterns of genetic diversity for a range-restricted stonefly imperiled by climate change. This finding included a history of divergence with gene flow, an unexpected conclusion for a mountaintop species. Beyond *L. tumana*, this study demonstrates the complexity of assessing genetic structure for weakly differentiated species, shows the degree to which rare alleles and missing data may influence results, and

highlights the usefulness of genome-scale data to extend population genetic inquiry in non-model species.

KEYWORDS
alpine stream ecology, coalescent, conservation genetics, Glacier National Park, global climate change, genetic structure, *Lednia tumana*, phylogeography, population genomics

1 | INTRODUCTION

For species facing rapid environmental change, making predictions about future population persistence benefits from insight into the magnitude and distribution of genetic diversity and the evolutionary forces shaping it. Generally, populations threatened by environmental change have three options: adapt in situ through phenotypic plasticity or genetic means, track suitable habitats through migration, or be extirpated (Hoffmann & Sgrö, 2011). Persistence through adaptation or phenotypic plasticity depends on contemporary levels of genetic variation (i.e. the template for evolutionary change), past environmental variation and subsequent selection and connectivity among critical habitats (e.g. the likelihood of an adaptive allele spreading as habitats shift). Thus, better understanding of genetic structure, patterns of diversity and evolutionary histories can inform predictions of the future viability of populations and species. Moreover, discriminating recent changes in population structure and demography from historical patterns can illuminate the impact of recent environmental change on genetic variation. Combined, these perspectives translate to a greater understanding of how genetic variation is shaped through time, a foundation for predicting response to future scenarios of global change, and more informed conservation decisions for species at risk of climate-change-induced extinction.

Perhaps nowhere are species facing more rapid change than above the permanent tree line in alpine, meltwater-influenced streams (Brown, Hannah, & Milner, 2007; Hotaling, Finn, Giersch, Weisrock, & Jacobsen, 2017). In these habitats, climate change is progressing at two to three times the global average (Hansen et al., 2005) causing major reductions of meltwater sources and significant changes to stream hydrology, biogeochemistry and channel stability (Hotaling, Hood, & Hamilton, 2017; Milner, Brown, & Hannah, 2009). With significant environmental variation over small geographical scales (e.g. <1 km), alpine streams provide critical habitat for an array of range-restricted communities (Hotaling, Finn, et al., 2017; Ward, 1994). This unique habitat distribution is largely due to variation in primary hydrological sources—whether glacier melt, snowfield melt, or groundwater-fed spring—and their influence on downstream conditions. Environmental heterogeneity is a major contributor to alpine headwaters harbouring significant beta diversity (i.e. biological differentiation among sites), both in terms of species and genetic diversity (Finn, Khamis, & Milner, 2013; Giersch, Hotaling, Kovach, Jones, & Muhlfeld, 2016; Hotaling, Hood, et al., 2017; Jordan et al., 2016). Consequently, a major predicted effect of climate change is the loss of this variation as glaciers recede and headwaters become more homogenous (Hotaling, Finn, et al., 2017; Jacobsen, Milner, Brown, & Dangles, 2012).

The impending threat of glacial recession on alpine stream ecosystems and biodiversity is exemplified in Glacier National Park (GNP), where remaining glaciers and permanent snow masses are predicted to disappear by 2030 (Hall & Fagre, 2003). The meltwater stonefly, *Lednia tumana* (Plecoptera: Nemouridae; Ricker, 1952), is endemic to GNP and surrounding areas and has been recommended for listing under the U.S. Endangered Species Act due to climate-change-induced habitat loss (U.S. Fish and Wildlife Service, 2016). *Lednia tumana* inhabits short sections (~500 m) of cold, meltwater streams directly below glaciers, permanent snowfields and groundwater-fed springs (Giersch et al., 2016; Muhlfeld et al., 2011). As glaciers and permanent snowpack decline, *L. tumana*'s range is expected to contract by more than 80% (Giersch et al., 2016; Muhlfeld et al., 2011). Historical and contemporary patterns of genetic diversity and demographic history for *L. tumana* however, remain explored. Mitochondrial DNA (mtDNA) evidence indicates low genetic diversity and significant subdivision across its range (Jordan et al., 2016), a pattern similar to other mtDNA-based population genetic studies of other alpine stream macroinvertebrates (Finn et al., 2013). However, given the limited resolution of mtDNA as a population-level marker (Macher et al., 2015), and the need to address metrics beyond population differentiation, genome-wide data are well-suited to this study system.

Recent advances in DNA sequencing and marker discovery (e.g. restriction-site associated DNA sequencing [RADseq]) have revolutionized the collection of genome-scale population genetic data for non-model species (Andrews, Good, Miller, Luikart, & Hohenlohe, 2016; Miller, Dunham, Amores, Cresko, & Johnson, 2007), enhancing the ability of researchers to measure genetic diversity and characterize evolutionary processes (Excoffier, Dupanloup, Huerta-Sánchez, Sousa, & Foll, 2013). Moreover, methods leveraging the site frequency spectrum (SFS) provide new opportunities to statistically test models of demographic history from genome-wide single nucleotide polymorphism (SNP) data (Excoffier et al., 2013; Gutenkunst, Hernandez, Williamson, & Bustamante, 2009). Using the SFS simplifies genome-wide patterns of genetic variation, while retaining signatures of demographic history, thereby providing a powerful tool for historical inference (Sousa & Hey, 2013). However, large SNP data sets also introduce novel challenges, particularly from an analytical perspective. RADseq (and similar) data sets can be filtered (and interpreted) in many different ways. Typically, filtering schemes focus on

the inclusion or exclusion of rare alleles and scale of missing data, as both can influence important study objectives, such as the identification of population structure (Babron, Tayrac, Rutledge, Zeggini, & Génin, 2012; Baye et al., 2011; Chattopadhyay, Garg, & Ramakrishnan, 2014). Congruence of population structure results across filtered data sets provides evidence for robust conclusions regarding the number of genetic clusters, and these results are easily obtained when clusters are highly differentiated with limited gene flow. However, for weakly differentiated groups—those that have recently diverged or are experiencing ongoing gene flow—the effects of filtering may be more profound, with greater need to explore how rare alleles and missing data impact population structure results.

In this study, we investigated the genetic structure and demographic history of *L. tumana* using a genome-wide SNP data set. Specifically, we quantified genetic diversity and assessed population structure across *L. tumana*'s range, and then incorporated these results into a series of demographic model tests to identify the best-fitting population history for *L. tumana*. Given the complex glacial history of GNP and the surrounding area (Carrara, 1987; Hall & Fagre, 2003), we tested a wide range of demographic models to characterize historic and contemporary forces shaping genetic diversity. Because our initial perspectives on population structure yielded unexpected results (i.e. more clusters identified than localities sampled), we took this result as an opportunity to explore the influence of singletons, amount of missing data and total number of SNPs for assessing population structure and connectivity. Collectively, this study provides genomic insight into the demographic history of an organism directly tied to declining glacial mass as well as a broadly applicable empirical example of how data filtering, and particular the presence or absence of singleton alleles, can influence assessments of population genetic structure.

2 | MATERIALS AND METHODS

2.1 | Genetic sampling

We collected 96 larval specimens of *L. tumana* from 10 streams (11 sites) throughout GNP and the surrounding areas between July 2010 and September 2011 (Figure 1a; Table 1). Localities were from independent streams except for two sites along Clements Creek, denoted as "high" and "low." All major alpine stream types (glacial, snowmelt and groundwater-fed spring) were represented in our sampling (Figure 1). Samples were stored in >80% EtOH and DNA was extracted using a Qiagen DNEasy Blood and Tissue Kit.

2.2 | RAD sequencing and SNP calling

RADseq libraries were prepared following a modified version of published protocols (Appendix S1; Baird et al., 2008; Miller et al., 2012). Briefly, samples were sonicated to 500 base pair (bp) fragments and size-selected using Agencourt AMPure XP beads (Beckman Coulter). Restriction digests used a single enzyme, SbfI. To uniquely mark each sample, we used six-base barcode adapters, each differing by at least three nucleotides. The final 96-sample RADseq library was sequenced on one lane of an Illumina HiSeq 2500 to produce 100 bp, single-end reads.

Raw reads were demultiplexed and RADseq loci were assembled using several modules of the STACKS 1.13 pipeline (Catchen, Amores, Hohenlohe, Cresko, & Postlethwait, 2011; Catchen, Hohenlohe, Bassham, Amores, & Cresko, 2013). Briefly, loci were assembled de novo in "ustacks" with a maximum distance between stacks of 2 and minimum read depth of 5. To maximize shared SNPs across individuals, we first filtered our data to remove individuals with >60% missing data. We then removed specific loci with >25% missing data, resulting in a final data set of 65 individuals from eleven localities (Table 1). All post-Stacks filtering steps and calculations of genotyping rate per individual for the final data set were performed in PLINK (Purcell et al., 2007). Tajima's *D* was calculated in δaδi 1.6.3 (Gutenkunst et al., 2009). At many stages of our analyses, we used PGDSPIDER 2.0.5.1 (Lischer & Excoffier, 2012) to convert data sets into program-specific formats. Additional details regarding read processing and SNP calling are provided in the Supporting Information.

2.3 | Testing for loci under selection

To ensure the neutrality of markers in our 6,819 SNP data set, we tested for outlier loci using BAYESCAN 2.1 (Foll & Gaggiotti, 2008). BAYESCAN uses a Bayesian model to estimate the likelihood that a given marker is under selection given the background differentiation (among populations), whereas accounting for differences in allele frequency due to small and/or varying sample sizes. We performed BAYESCAN analyses using default settings in two ways: (1) sampling localities and (2) for each genetic cluster (see Results). Outlier loci were identified as those that exceeded a false discovery rate of 0.05.

2.4 | Population structure and differentiation

Population genetic structure was inferred using a Bayesian clustering method implemented in the program ADMIXTURE 1.3.0 (Alexander, Novembre, & Lange, 2009) and a discriminant analysis of principal components (DAPC) implemented in the R package "adegenet" (Jombart, 2008; Jombart, Devillard, & Balloux, 2010). We were also interested in how various aspects of data filtering (i.e. presence or absence of singletons) and missing data affected results. To provide a systematic perspective on these factors, we generated five data sets for population structure analysis. These included: (1) the full 6,819 SNP data set described above (~11% missing data overall); (2) a 2,733 SNP data set with all singletons removed, which was roughly equivalent to a minor allele frequency cut-off of 0.015 for 65 individuals (~11% missing data overall); (3) a 1,467 SNP data set with all singletons and any locus with >10% missing data removed (~5% missing data overall); (4) a 761 SNP data set with all singletons and any SNP with >5% missing data removed (~3% missing data overall); and, (5) an 86 SNP data set with all singletons removed and no missing data. All five of these data sets were analysed using both ADMIXTURE and DAPC as described below.

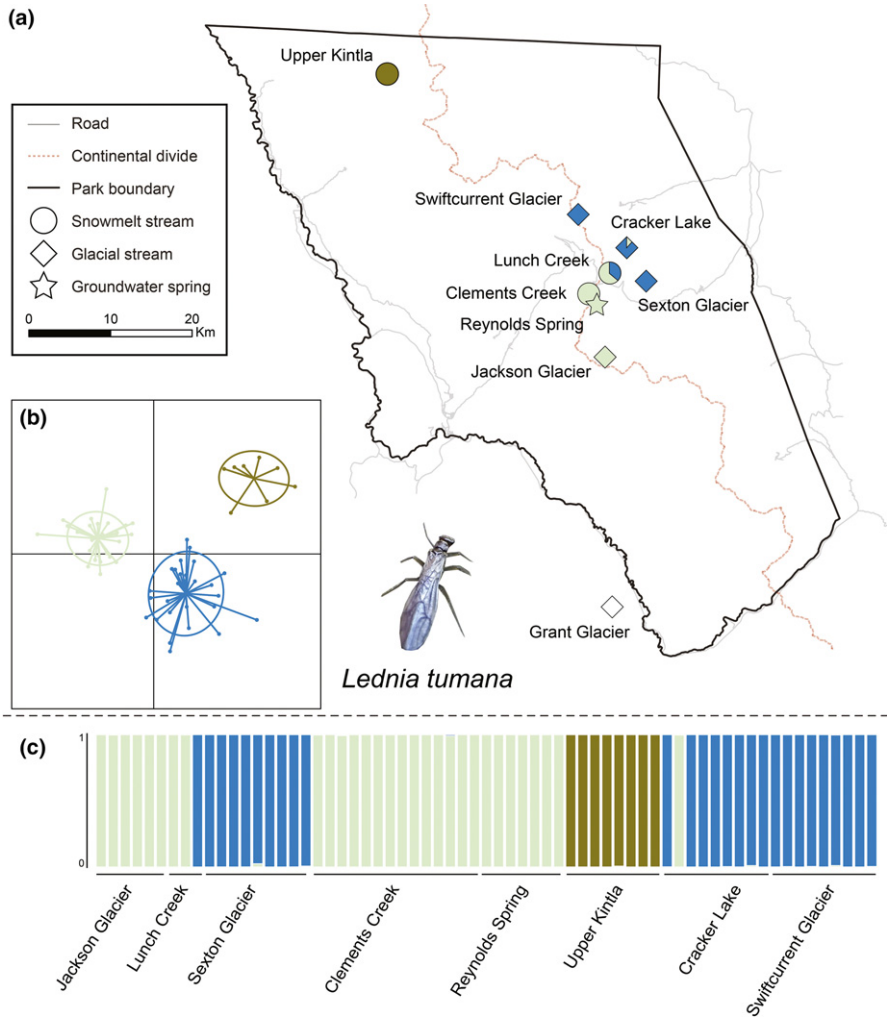

FIGURE 1 (a) Sampling localities across *Lednia tumana*'s known range within and near Glacier National Park, Montana, USA. Symbol shapes correspond with primary hydrological source and colours indicate assignment to genetic clusters. The white triangle for Grant Glacier indicates a sampled population from which too few specimens passed filtering to be included in downstream analyses. (b) Results of a discriminant analysis of principal components (DAPC) for $K = 3$ clusters. (c) DAPC-based assignment probabilities for all samples included in a 1,467 SNP data set with all singleton alleles removed and ~5% missing data [Colour figure can be viewed at wileyonlinelibrary.com]

TABLE 1 Sampling and locality information for population genomic and demographic history analyses of *Lednia tumana* in and near Glacier National Park, Montana, USA. The number of individuals (*n*) is given for the total number sequenced per locality and the number of individuals retained in the post-filtering 6,819 SNP data set

Locality	GPS coordinates	Elevation (m)	*n*, initial	*n*, post-filtering
Grant Glacier[a]	48°19′45.37″, −113°44′28.10″	1,836	3	0
Jackson Glacier	48°36′19.97″, −113°41′44.65″	2,006	7	6
Lunch Creek	48°42′35.40″, −113°42′15.28″	2,285	15	3
Sexton Glacier (main)	48°42′1.48″, −113°37′24.12″	1,847	9	4
Sexton Glacier (south)	48°41′58.33″, −113°37′20.33″	1,827	9	5
Clements Creek (high)	48°41′24.07″, −113°44′0.95″	2,173	9	8
Clements Creek (low)	48°41′16.33″, −113°43′43.11″	2,045	9	6
Reynolds Spring	48°41′4.77″, −113°43′35.05″	2,082	8	7
Upper Kintla	48°56′48.44″, −114°8′24.59″	1,826	9	8
Cracker Lake	48°44′21.42″, −113°39′11.99″	1,867	9	9
Swiftcurrent Glacier	48°46′41.52″, −113°45′21.36″	2,010	9	9
		Total	96	65

[a]Not included in downstream analyses due to limited coverage after filtering.

Admixture analyses were performed using default settings for a range of cluster numbers (K) between 1 and 12. For each K, we calculated and plotted the cross-validation error to select the best-fit (lowest cross-validation error) K. For DAPC analyses, we first used the *find.clusters* function to assess the optimal number of groups using the Bayesian information criterion (BIC), with lowest BIC corresponding to the best-fit K. We retained the optimal number of principal components according to the α-score for each data set to avoid overfitting

the population structure model (Jombart et al., 2010). Next, we performed a final DAPC analysis for each data set using the best-fit K and optimal number of discriminant functions retained.

We calculated pairwise F_{ST} among sampling localities, tested for isolation-by-distance (Wright, 1943), and performed a hierarchical AMOVA for the 1,467 SNP data set using the program GENODIVE 2.0b27 (Meirmans & Van Tienderen, 2004). For pairwise F_{ST} calculations, significance was assessed using 5,000 permutations (or resamplings) of the observed data. We conducted a series of Mantel tests to test for correlation between geographic and genetic distance (F_{ST}). To calculate geographical distances, we took the natural log of Euclidean distances among sampling localities estimated in Google Earth. The first Mantel test included all pairwise comparisons among sampling localities. To take the spatial dependence of the data into account (Meirmans, 2012), two additional Mantel tests were conducted for only those sampling localities within identified the "south" and "central" genetic clusters (see Results). No Mantel test was conducted for the "north" cluster because it only contained one sampling locality. All Mantel tests were performed using "adegenet" (Jombart, 2008; Jombart et al., 2010) and 9,999 permutations. The hierarchical AMOVA was performed on our best assessment of hierarchical population structure (K = 3, see Results and Discussion) to quantify how genetic variation was partitioned across different levels of sampling.

2.5 | Demographic model testing

We sought to understand how *L. tumana*'s demographic history has changed in a temporal framework, including the roles of isolation and migration. These demographic models were developed around a K = 3 level of population structure, which we identified as the most likely scenario for population structure based on our thorough exploration of data filtering and missing data (see additional details below). These genetic clusters generally corresponded with geography and we refer to them as north, central and south. Populations were assigned to genetic clusters based upon the majority genetic assignment of individuals sampled.

We tested 20 demographic models (Figure 2). Detailed model schematics are included in Figures S1 & S2 with model-specific definition files in Appendix S2 of the Supporting Information. Briefly, models included scenarios specifying two divergence events for all possible topologies of the three genetic clusters (models 1–3, 8–13), trifurcation models where extant genetic clusters emerged simultaneously from a common ancestor (models 7 & 14) and models where admixture between two existing genetic clusters created the third (models 4–6, 15–20). For all models, we varied the potential for bidirectional gene flow both historically and recently.

We selected and parameterized the best-fit demographic model using fastsimcoal2 v2.5.2 (Excoffier et al., 2013), a coalescent-based program which estimates demography from the SFS. Since demographic inference from the SFS is particularly dependent on the presence of rare alleles (i.e. singletons and doubletons; Gutenkunst et al., 2009), we used the full 6,819 SNP data set for all demographic modelling analyses but only one randomly selected SNP per RADseq locus. Our fastsimcoal2 analyses followed an initial set of model selection runs, comparison of maximum observed and expected likelihoods to select the best-fit model, then subsequent parameter estimation through simulation of new SFSs for the best-fit model, followed by parametric bootstrapping. For complete details regarding model selection and parameterization, see "fastsimcoal2 analyses" in the Supporting Information.

To account for the diploidy of *L. tumana*, we divided the haploid fastsimcoal2 parameter estimates in half. Estimates of divergence time in fastsimcoal2 are calculated as number of generations before present. Field observations of co-occurring mature, late-instar nymphs and smaller, early-instar nymphs (S.H., personal observation) suggest a 2-year life cycle. Therefore, we doubled divergence time estimates to convert from generations to years.

3 | RESULTS

3.1 | RADseq data

We generated 201,634,318 total sequence reads with variation in reads per individual (avg. = 1,012,499; min. = 2497; max. = 2,901,467). We identified 92,657 total RADseq loci using all 96 samples. After the overall filtering steps were completed, our final data set contained 65 samples, 3,680 variable RADseq loci and 6,819 SNPs (mean = 1.85 per locus). Within this final dataset, 4,043 SNPs were singletons (minor allele count = 1). The genotyping rate (i.e. percentage of all genotyped sites without missing data) for the full 6,819 SNP data set was 89.0%. F_{ST}-outlier tests identified six outliers in the full data set (Figure S3) and none when genetic clusters (see below) were accounted for. Given this small percentage (<0.01%) and lack of outliers when accounting for regional genetic clusters, we did not remove these outlier SNPs from downstream analyses.

3.2 | Population structure

Across all five data sets with varied filtering criteria, Admixture analyses favoured grouping all samples into a single genetic cluster based on cross-validation scores (Figure S4). In contrast, DAPC results detected population structure, with the optimal number of genetic clusters heavily influenced by singletons, missing data and the total number of analysed SNPs (Figure 3). Analysis of the full 6,819 SNP data set produced BIC scores that identified K = 12 as the optimal number of genetic clusters. When singletons were removed (2,733 SNP data set), BIC values indicated a K = 5 as the optimal level of structure. When the amount of missing data was trimmed to ~5% (1,467 SNPs) or 3% (761 SNPs), the BIC identified K = 3 as optimal. Finally, for the 86 SNP data set featuring no singletons and no missing data, the lowest BIC corresponded to a K = 4.

On the basis of these results (and geography), we identified K = 3 as the best estimate of population structure (see Figure 3 and the Discussion for full justification of this decision). Briefly, we made this decision because K = 3 clusters was statistically supported by two subsampled data sets and represented the most conservative,

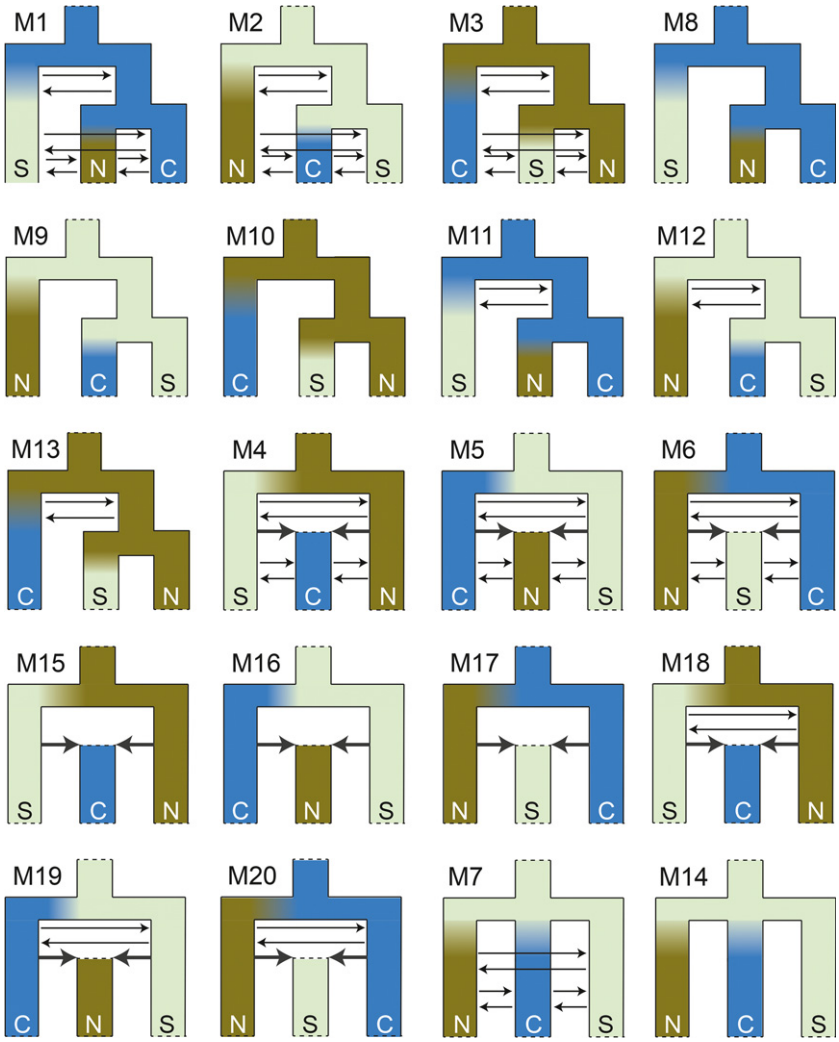

FIGURE 2 Schematics of the 20 demographic models compared in this study. Large arrows indicate admixture events, small arrows represent the presence of gene flow and colours correspond to genetic clusters as defined in population structure analyses. Ancestral colours were arbitrarily defined for simplicity and model numbers reflect the order in which they were constructed (and the order of results in Table 5) [Colour figure can be viewed at wileyonlinelibrary.com]

biologically appropriate number of clusters versus the limited support we observed for other *K*'s. Moreover, given the known impact of rare alleles on population structure (e.g. Babron et al., 2012) favouring $K = 3$ over the $K = 12$ DAPC result when singletons were included is a reasonable decision. Identified genetic clusters largely aligned with geography and resulted in a "north" cluster including Upper Kintla samples only, a "central" cluster including samples from Swiftcurrent Glacier, Cracker Lake and Sexton Glacier and a "south" cluster, including samples from Lunch Creek, Clements Creek, Reynolds Spring and Jackson Glacier (Figures 1, 3 & 4).

3.3 | Population differentiation and gene flow

Mean pairwise genetic differentiation (F_{ST}) among localities was 0.033 ($SD = 0.016$), and ranged from 0 (both sites along Clements Creek compared to one another) to 0.067 (Sexton Glacier [main] to Upper Kintla; Table 2). On average, the least differentiated locality from all others sampled was the higher elevation site along Clements Creek (mean $F_{ST} = 0.025$) and the most differentiated locality, Upper Kintla (mean $F_{ST} = 0.051$; Table 2), was also the most geographically separated, suggesting a possible pattern of isolation-by-distance. Indeed, we detected a positive association between genetic and geographical distances (Mantel's $r = .72$, $p = .003$). However, when population structure was accounted for in subsequent Mantel tests, the results were less conclusive. For "central," the signal of isolation-by-distance was stronger than the overall pattern (Mantel's $r = .92$, $p = .04$), but for "south," the observed pattern was both weaker and not significant (Mantel's $r = .5$, $p = .22$). AMOVA results identified modest differentiation among the three genetic clusters ($F_{CT} = .020$, $p < .0001$; Table 3), but this only accounted for 2.0% of the total variation. Variation among localities within groups was also significantly differentiated (Table 3), and this also explained a low amount of the total variation (3.6%). Most of the observed variation (94.3%) was among individuals within sampling localities (Table 3).

For the full 6,819 SNP data set, the number of private alleles (PAs; those observed in only one locality) varied widely (Table 4), with Cracker Lake averaging the most per sample (215.7) and Clements Creek (high) the least (25.3). Excluding intrastream comparison, the lowest number of PAs per sample was observed for Swiftcurrent Glacier (37.2) and Reynolds Creek (38.4). We note that total numbers of PAs did not appear to be a product of variation in sequencing effort as Cracker Lake samples did not have exceptionally high numbers of average reads per sample. For the full 6,819

(a) **6819 SNPs.** Removed loci: none. ~11% missing overall (*K* = 12)

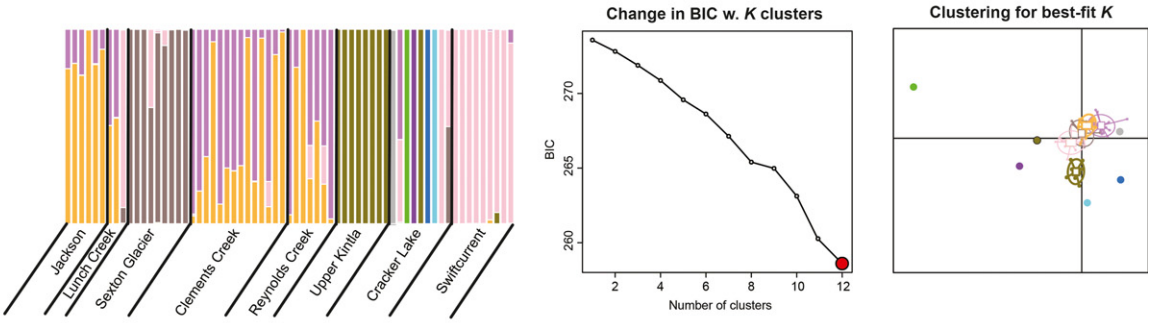

(b) **2733 SNPs.** Removed loci: MAC = 1. ~11% missing overall (*K* = 5)

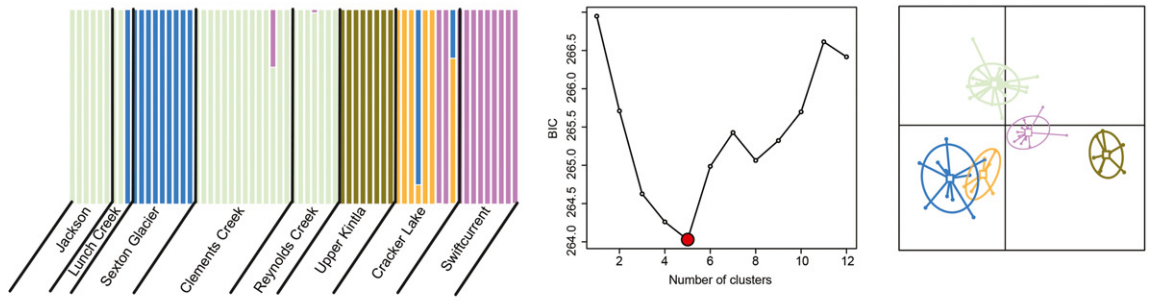

(c) **1467 SNPs.** Removed loci: MAC = 1, >10% missing. ~5% missing overall (*K* = 3)

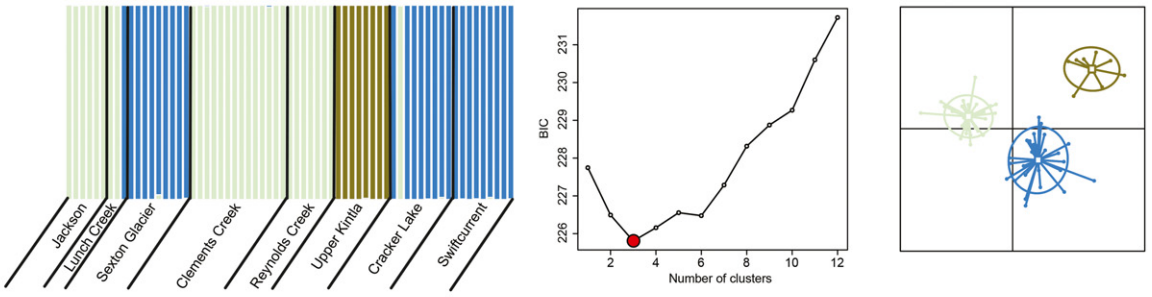

(d) **761 SNPs.** Removed loci: MAC = 1, >5% missing. ~3% missing overall (*K* = 3)

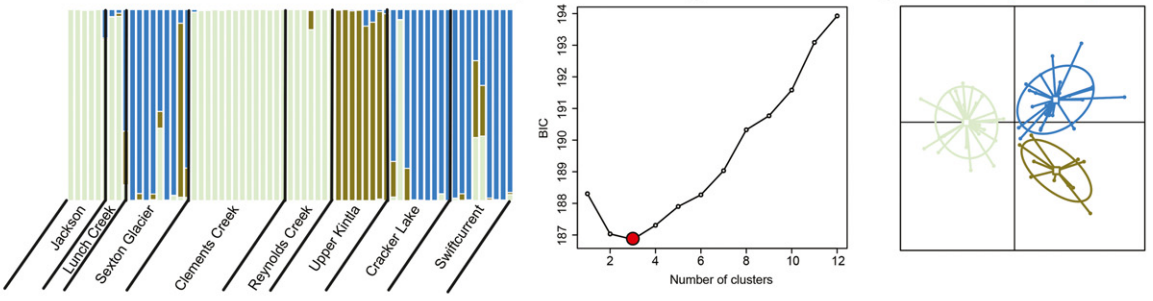

(e) **86 SNPs.** Removed loci: MAC = 1, >0% missing. No missing data (*K* = 4)

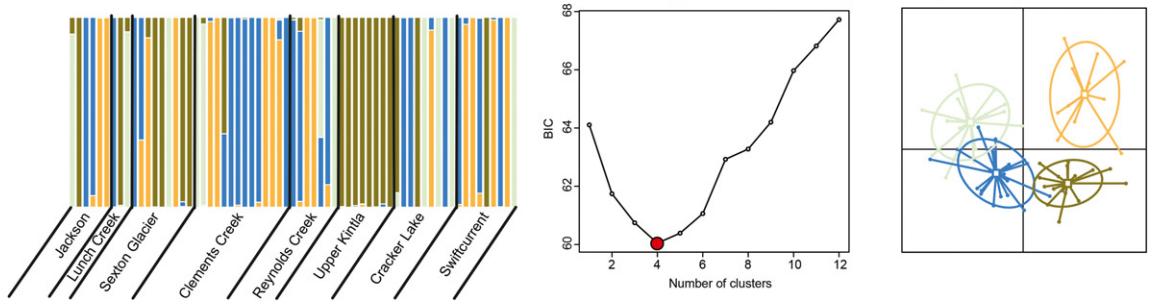

FIGURE 3 Comparisons of population structure in *Lednia tumana* inferred from DAPC analyses for five data sets with varying numbers of SNPs included. Filters are as described for each set of plots. MAC = 1: minor allele count of 1 (i.e. singletons) removed. The best-support *K* is in red. From right to left for each comparison: assignment plots where each vertical bar represents one individual, a plot of the Bayesian Information Criterion (BIC) for a range of *K* values (lower BIC indicates higher model support) and individual assignments to genetic clusters based upon the two most informative principal components [Colour figure can be viewed at wileyonlinelibrary.com]

SNP data set, nucleotide diversity was highest in Cracker Lake samples (π = 0.119) versus the total average (π = 0.087; Table 4). Overall, Tajima's *D* was −2.26, suggesting a history of population expansion. For each genetic cluster, *D* was still negative, ranging from −0.25 to −1.58. The greatest magnitude of *D* for individual localities was observed for Cracker Lake (−1.40; Table 4).

For the 6,819 SNP data set, an interesting pattern was observed where H_{obs} was consistently lower than H_{exp} when calculated for localities, but reversed ($H_{obs} > H_{exp}$) when calculated for genetic clusters (aside from Upper Kintla which was the only locality in the north cluster; Table 4). However, when singletons were removed and missing data reduced to 10% (i.e. the 1,467 SNP data set), H_{obs} was consistently lower than H_{exp} at both the level of sampling localities and regional cluster (Table S1).

3.4 | Demographic model selection and parameter estimation

Demographic model testing revealed model M1 to best fit our data (Figure 5, Table 5; model likelihood = 0.96). Model M1 included an initial divergence between the south and central+north genetic clusters, followed by a subsequent divergence between the central and north clusters with a bidirectional gene flow through *L. tumana*'s history. All other models, including those similar to M1, but with more restricted gene flow, were poorly supported (ΔAIC ≥6.86; model likelihoods ≤3.1E-2; Table 5).

Point estimates of demographic parameters for model M1 are provided with 95% CIs (Figure 5; Table S4). Our results lend support to population expansions for all genetic clusters, with current effective population sizes (N_e) ranging from 246,743–410,562 (83,549–674,997), which tend to be much higher than estimates for both the ancestor of all localities, $N_e^{N\_ANCALL}$, at 44,425 individuals (40,037–398,531) and the ancestral north+central cluster, $N_e^{N\_ANC01}$, estimated at 12,637 individuals (1,498–30,490).

When accounting for ploidy and generation time, divergence time point estimates were all less than 20,000 years ago (ya) with the ancestral north+central cluster splitting from South 17,551 ya (14,734–223,599), and north subsequently diverging from central 13,314 ya (10,751–15,450). Estimates of migration probabilities per generation between regional clusters varied greatly with the highest

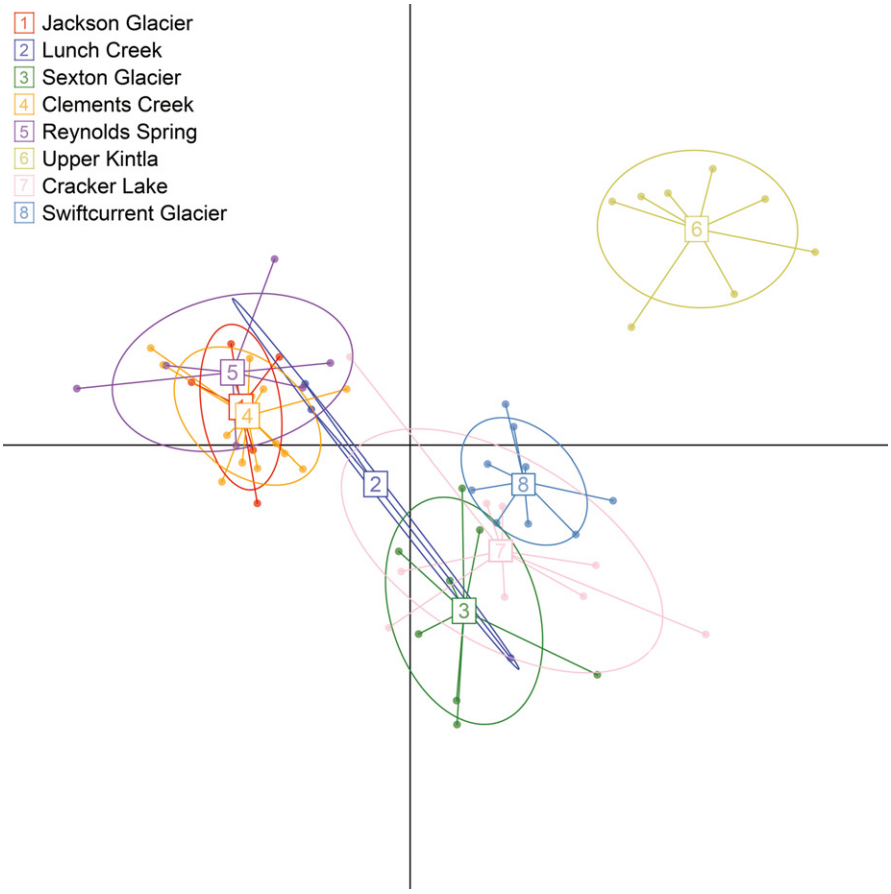

FIGURE 4 Results of a discriminant analysis of principal components for *K* = 3 clusters and all eight streams included in demographic modelling of *Lednia tumana*. Each point represents one sample and points are colour-coded to sampling locality (streams). Note that this is the same clustering pattern presented in Figure 1b, except here, samples are coded by stream rather than genetic cluster. Samples belonging to clusters 2 (Lunch Creek) and 7 (Cracker Lake) highlight immigration between the south and central clusters [Colour figure can be viewed at wileyonlinelibrary.com]

TABLE 2 Population differentiation (F_{ST}) among localities calculated for the 1,467 SNP data set for *Lednia tumana*. Values not significant at $p \leq .05$ are in bold. Mean values represent the average F_{ST} for each location (corresponding with associated columns). Average F_{ST} overall was 0.033. Locality abbreviations: JKG = Jackson Glacier, LCK = Lunch Creek, SGM = Sexton Glacier (main), SGS = Sexton Glacier (south), CCL = Clements Creek (low), CCH = Clements Creek (high), REY = Reynolds Spring, KLA = Upper Kintla, CKL = Cracker Lake, SWG = Swiftcurrent Glacier

	JKG	LCK	SGM	SGS	CCL	CCH	REY	KLA	CKL	SWG
JKG	–	0.046	0.045	0.033	0.018	0.011	**0.001**	0.055	0.034	0.037
LCK		–	0.056	0.024	0.026	0.028	0.034	0.058	**0.020**	0.048
SGM			–	**0.008**	0.047	0.054	0.051	0.067	0.019	0.033
SGS				–	0.035	0.032	0.033	0.055	0.021	0.033
CCL					–	**0**	**0.004**	0.046	0.027	0.026
CCH						–	**0.006**	0.053	0.028	0.030
REY							–	0.047	0.030	0.028
KLA								–	0.040	0.036
CKL									–	0.025
SWG										–
Mean	0.031	0.038	0.042	0.030	0.025	0.027	0.026	0.051	0.027	0.033

probabilities observed for north into south, 3.30E-5 (9.61E-7–2.07E-4), and central into south, 1.11E-5 (3.12E-10–6.90E-5). Ancestral migration probabilities were lower in both directions, with migration from north+central into south at 5.33E-11 (1.88E-10–6.22E-10) and the reverse at 1.19E-8 (8.16E-10–9.95E-5). In this context, migration probability refers to the per generation likelihood that any gene from one population transfers to another. Changing the mutation rate influenced population size and divergence time estimates by a similar amount (i.e. a 10-fold increase in the mutation rate corresponded with a 10-fold decrease in parameter estimates; Table S4).

4 | DISCUSSION

4.1 | Characterizing population structure for a weakly differentiated alpine stonefly

Our best estimate of population genetic structure is that contemporary *L. tumana* populations comprise three genetic clusters that align with geography. We settled on this three-cluster model as the best fit for our data (Figures 1 & 3) after taking into account statistical support and clustering patterns across different data-filtering strategies. First, the lack of support identified by Admixture, and its stark contrast with the DAPC results, was in-line with other RADseq studies of poorly differentiated groups (e.g. lobsters; Benestan et al., 2015), suggesting that Admixture was likely to substantially underestimate population structure. Therefore, we focused on the DAPC results. Inspection of the $K = 12$ result from analysis of the 6,819 SNP data set identified six clusters that are made up of single Cracker Lake individuals. This result is a clear overestimation of population structure and appeared to be linked to the presence of singletons, which can influence population structure results (Babron et al., 2012). Indeed, this effect of singletons was further evidenced by the 2,733 SNP data set, where with singletons removed, the best-fit structure model dropped to a $K = 5$. Explorations of the effect of missing data by further filtering loci with greater than 10% missing data (1467 SNP data set) and 5% missing data (761 SNP data set) reduced the best-fit model to a $K = 3$. Interestingly, the $K = 5$ and $K = 3$ results were largely in agreement with one another, with the only difference being whether to group individuals from Sexton Glacier, Cracker Lake and Swiftcurrent Creek into three clusters (2,733 SNPs) or one (1,467 and 761 SNPs). Ordination plots for the $K = 5$ model indicated some amount of overlap between the Cracker Lake and Sexton Glacier localities, two of the most weakly differentiated localities ($F_{ST} = 0.019$–0.021 versus average $F_{ST} = 0.033$). On the other end of the spectrum, the removal of all missing data (86 SNP data set) produced a $K = 4$ result, but with substantial loss of information, as nearly every locality comprised individuals assigned to multiple clusters with uncertain assignments.

Missing data has been previously shown to influence population structure analyses (Chattopadhyay et al., 2014). Our results are consistent with this, although the effect is much weaker than singletons, and it appears there may be a bit of a sweet spot when it comes to identifying patterns of structure with regards to missing data. A slight reduction in missing data from 11% to 5% had the biggest effect on inference of *K*, with similar results achieved with the 3% data set (although with greater admixture or uncertainty in cluster assignments). It is possible that the general results here may be specific to this study system and data set. Nonetheless, we are confident in our choice to reject results based on the overall full data set and those from one in which all SNPs with any missing data are thrown out. Deciding between $K = 3$ or 5 was slightly more nuanced, and we elected to take a conservative approach in selecting the $K = 3$ model given the nestedness of the additional clusters identified in the $K = 5$ model in a single cluster of the $K = 3$ model.

Unlike studies focusing on wide-ranging and highly-differentiated species, we faced the challenge of identifying a best-fit model of

TABLE 3 Segregation of genetic variation in *Lednia tumana* according to an analysis of molecular variance (AMOVA) for 10 sampling localities (eight streams) in Glacier National Park grouped into three genetic clusters (north, central and south). The AMOVA was calculated for the 1,467 SNP data set with singletons removed and only loci with <10% missing data retained

Source of variation	Fixation index	Percentage of variation	*p*
Among clusters	F_{CT} = 0.020	2.00	<.0001
Among localities within clusters	F_{SC} = 0.037	3.62	<.0001
Within localities	F_{ST} = 0.056	94.38	<.0001

population structure without clear results. A lack of consensus in population structure across data sets and methods for large-scale SNP data sets is not unique to this study (e.g. Benestan et al., 2015), but it's still an understudied finding in a field dominated by clear expectations and results (but see Janes et al. [2017] discussion of studies underestimating *K* after an initial and clear *K* = 2 result). Specifically, our aim was to better understand how the full 6,819 SNP data set could give such opposing results when analysed via DAPC (*K* = 1) or ADMIXTURE (*K* = 12). While our results still do not provide a perfectly objective method for describing population structure among contemporary populations of *L. tumana*, they clearly support other studies which have shown how singletons can obfuscate the signal of population genetic structure (Babron

TABLE 4 Population genetic statistics calculated from the full 6,819 SNP data set of *Lednia tumana*. Statistics are provided for the sampling localities in Glacier National Park, genetic clusters and overall. Nucleotide diversity (π), expected heterozygosity (H_{exp}), observed heterozygosity (H_{obs}) and the inbreeding coefficient (F_{IS}) were calculated for variable positions only. Additional abbreviations include: PA = private alleles, *D* = Tajima's *D*. Similar statistics calculated for the 1,467 SNP data set which had all singletons removed and only retained loci with <10% missing data are provided in Table S1

	PA	PA per sample	*D*	π	H_{exp}	H_{obs}	F_{IS}
Sampling locality							
Jackson Glacier	334	55.7	−0.200	0.092	0.082	0.074	0.040
Lunch Creek	177	59.0	0.229	0.082	0.066	0.056	0.046
Sexton Glacier (main)	206	51.5	−0.040	0.087	0.075	0.068	0.038
Sexton Glacier (south)	253	50.6	−0.019	0.087	0.077	0.061	0.056
Clements Creek (low)	363	60.5	−0.107	0.093	0.085	0.073	0.052
Clements Creek (high)	201	25.3	0	0.086	0.078	0.070	0.037
Reynolds Creek	269	38.4	−0.072	0.091	0.083	0.071	0.050
Upper Kintla	410	51.3	−0.249	0.090	0.083	0.067	0.057
Cracker Lake	1,941	215.7	−1.404	0.119	0.111	0.084	0.097
Swiftcurrent Glacier	335	37.2	−0.104	0.087	0.081	0.070	0.046
Regional metapopulation							
North	410	51.3	−0.249	0.090	0.083	0.067	0.057
Central	2,180	77.9	−1.581	0.112	0.080	0.110	0.131
South	1,276	47.3	−0.791	0.108	0.084	0.105	0.104
Overall	n/a	n/a	−2.255	0.098	0.097	0.071	0.165

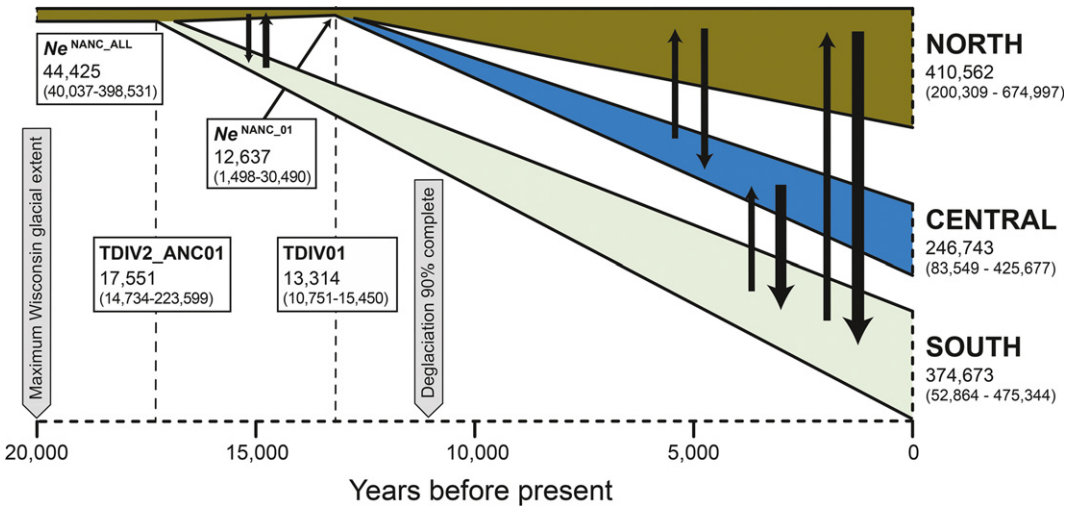

FIGURE 5 A schematic of the best-fit demographic model (Model 1) for *Lednia tumana*. Larger font parameter values are point estimates from the best-fit model selection replicate. Divergence time estimates are in years and effective population size estimates (Ne) are in numbers of individuals. Parentheses indicate 95% confidence intervals of parameter estimates. Black arrows represent relative estimates of migration probabilities with variation in arrow size based on a log scale. Ancestral coloration was arbitrarily chosen to simplify visualization. Geological reference points were taken from Carrara (1987) [Colour figure can be viewed at wileyonlinelibrary.com]

TABLE 5 Results of model selection analyses performed in FASTSIMCOAL2 for three genetic clusters of *Lednia tumana*. *p* = number of parameters in the model. Model numbers correspond to those in Figure 2

Model	Description	*p*	ΔAIC	Model probability
Divergence with gene flow (recent and historical)				
1	(North, Central), South	15	–	0.96
2	(Central, South), North	15	12.36	1.99E-3
3	(North, South), Central	15	19.27	4.81E-9
Divergence with no gene flow				
8	(North, Central), South	7	6.86	3.10E-2
9	(Central, South), North	7	28.46	6.33E-7
10	(North, South), Central	7	26.60	5.91E-7
Divergence with gene flow (historical only)				
11	(North, Central), South	9	9.92	6.73E-5
12	(Central, South), North	9	32.38	8.96E-8
13	(North, South), Central	9	33.14	6.11E-8
Admixture with gene flow (recent and historical)				
4	North and South diverged, Central admixed	13	40.06	1.92E-9
5	Central and South diverged, North admixed	13	27.34	1.11E-6
6	North and Central diverged, South admixed	13	32.19	9.82E-8
Admixture with no gene flow				
15	North and South diverged, Central admixed	7	27.59	9.81E-7
16	Central and South diverged, North admixed	7	23.23	8.68E-6
17	North and Central diverged, South admixed	7	28.79	5.37E-7
Admixture with gene flow (historical only)				
18	North and South diverged, Central admixed	9	30.51	2.27E-7
19	Central and South diverged, North admixed	9	27.26	1.15E-6
20	North and Central diverged, South admixed	9	32.92	6.83E-8
Trifurcation with gene flow				
7	All lineages diverged at the same time.	11	35.91	1.53E-8
Trifurcation with no gene flow				
14	All lineages diverged at the same time.	5	24.69	4.18E-6

et al., 2012; Baye et al., 2011). Moreover, our results align with other studies (e.g. Benestan et al., 2015) in showing Admixture to be limited in its power to detect structure among weakly differentiated groups. While there may well be additional structure within the central cluster, our identification of $K = 3$ also serves a practical purpose. For three genetic clusters, our demographic models already included 15 parameters (Table 5). A five-cluster model would include 49 parameters, greatly escalating the computational complexity of the study and reducing the likelihood of obtaining biologically meaningful results.

4.2 | Demographic history of *L. tumana*

Our results show that genetic structure, effective population size and genomic variation in *L. tumana* likely accumulated over the last 20 kyr, likely in response to a changing, post-Pleistocene environment. Among the three identified geographic genetic clusters, the deepest divergence occurred ~17 ka and corresponds with the initial stages of ice retreat following the Wisconsin glaciation in northwestern Montana (*c.* 20 ka; Carrara [1987]). This was followed by a second divergence ~4 kyr later between the present-day north and central clusters, a result that aligns well with a south-to-north pattern of ice sheet recession. Indeed, during this time glacial ice was receding across north-western Montana, including GNP (Carrara, 1987), and divergence time estimates match well with the likely opening of new glacial stream habitat and its subsequent colonization by *L. tumana* from refugia. Moreover, while important assumptions must be considered when interpreting the temporal estimates presented here (see "Limitations to empirical estimates of demographic history from genome-scale data" in Supporting Information), our results provide vital insight into how south-to-north ice sheet recession at the end of the Pleistocene influenced patterns of genetic variation for an alpine species directly tied to meltwater sources.

Several additional lines of evidence support the hypothesis that extant genetic clusters of *L. tumana* originated and expanded from post-Pleistocene refugia. First, N_e estimates for ancestral nodes were substantially smaller than those for present-day regional

clusters (Figure 5; Table S3). Second, Tajima's *D* calculated for all genetic clusters was negative, which indicates that each may have experienced a recent population expansion. While the magnitude of these Tajima's *D* estimates is below the generally accepted threshold of a "significant" *D* ($\geq|\pm 2|$) for a population expansion, when calculated for the full data set, *D* was −2.255, as often expected when pooling subpopulations (Table 4). A rise in N_e may also be the product of undiagnosed additional population structure within identified genetic clusters (perhaps within the difficult-to-tease-apart central cluster described above). Greater population sampling that fully reflects our current understanding of *L. tumana* distribution (see Giersch et al., 2016) could help to resolve this.

Interestingly, one sampling locality within the central cluster, Cracker Lake, contained a disproportionately high number of private alleles (Table 4). While these PAs could be the product of sequencing error or elevated sequencing coverage, this is unlikely as similar excess was not observed for other localities (and we have no evidence for higher sequencing effort or lower genotyping quality for Cracker Lake). An alternate, biotic explanation is that a large and expanding N_e in the Cracker Lake population (perhaps at a faster rate than other sampled localities) has led to an accumulation of younger haplotypes and an excess of low-frequency alleles. This alternate explanation is supported by the geology of Cracker Lake, with the Siyeh Glacier feeding the stream containing *L. tumana* surrounded by a horseshoe of 2,400 m walls, likely limiting gene flow between Cracker Lake and nearby populations.

4.3 | Alpine aquatic biodiversity: an uncertain future

As climate change proceeds and alpine landscapes change, the need for accurate predictions of how species will respond becomes increasingly pressing. Understanding the potential for migration among populations is an important component of this discussion (Hoffmann & Sgrò, 2011). For alpine stream taxa, gene flow is challenged by fragmentation of suitable habitats, often resulting in population isolation and increased probability of extirpation (Hotaling, Finn, et al., 2017). These expectations are supported by several mtDNA studies identifying strong isolation among headwater macroinvertebrate species (e.g. Monaghan, Spaak, Robinson, & Ward, 2001), including *L. tumana* (Jordan et al., 2016). However, this study is the first to use genomic tools to understand historical and contemporary patterns of genetic diversity and connectivity in a range-restricted endemic that is acutely vulnerable to climate-change-induced loss of meltwater habitat.

With the addition of genomic data, demographic model testing unequivocally favoured a history of gene flow over models that either excluded migration fully, or included fewer migration parameters. Both morphological (Garcia-Raventós, Viza, Tierno de Figueroa, Riera, & Múrria, 2017) and mtDNA (Finn & Adler, 2006; Finn, Encalada, & Hampel, 2016; Giersch et al., 2016; Jordan et al., 2016) evidence suggests that stoneflies (and related alpine stream species) are poor dispersers. Consequently, the support for gene flow occurring on large spatial scales is surprising and may provide some degree of optimism from a climate change perspective. Species exhibiting population structure with ongoing gene flow may be at an advantage in their response to climate change as potentially adaptive genetic variation from one geographical area or habitat type may spread to another (Hoffmann et al., 2015). *Lednia tumana* appears to meet both criteria (population structure and ongoing gene flow), thus indicating that it at least has the potential for an adaptive response to changing climate. Indeed, as a glacially tied stream insect, *L. tumana* is representative of a global aquatic community that is directly at risk due to climate-change-induced habitat loss (Giersch et al., 2016; Hotaling, Finn, et al., 2017; Hotaling, Hood, et al., 2017; Muhlfeld et al., 2011).

4.4 | Future directions and conclusions

Ultimately, to form a comprehensive understanding of the evolutionary potential and persistence of *L. tumana* under future warming scenarios, additional studies will be required. This future research should include specific assessments of the role of isolation-by-distance (Wright, 1943) versus isolation-by-environment (Wang & Bradburd, 2014) in shaping extant genetic diversity, targeted efforts to identify ecologically relevant genetic diversity that may be under selection (at a much finer genomic scale than in this study), and robust estimations of gene flow between streams, with a specific focus on those populations inhabiting opposite ends of the habitat spectrum. In all of this, it will remain important to not discount the role of phenotypic plasticity as a mechanism for population persistence as glaciers decline. A plastic response could act as an initial buffer, allowing populations to persist outside of their environmental optima while genetic adaptation accumulates (Reusch, 2014). To this end, laboratory tests of thermal tolerance for *L. tumana* nymphs from a single stream (the snowmelt-fed Lunch Creek) suggested they can tolerate much warmer conditions than they experience in the wild (Treanor, Giersch, Kappenman, Muhlfeld, & Webb, 2013). Most importantly, the survival of communities cannot be inferred from a single species. To better resolve the potential for glacially tied communities to persist in a rapidly changing landscape, insight from a combined, multi-taxon perspective is required (Hotaling, Finn, et al., 2017).

Despite the challenges associated with predicting the future of alpine stream taxa, this study demonstrates the promise of genomic tools for moving beyond patterns of genetic differentiation to also include robust estimates of demographic history. Specifically, we showed the utility of genome-wide information to resolve population structure and recent demographic history for an alpine stonefly at high risk of local extirpation as climate change proceeds (Giersch et al., 2016). As alpine stream species are facing similar threats globally, the results of this study have implications far beyond *L. tumana* or GNP. Indeed, studies like ours can easily be conducted for other species with no genomic resources to help quantify, monitor and predict changes in population structure, connectivity and ultimately persistence, in the face of environmental change.

ACKNOWLEDGEMENTS

This work was funded by the USGS Northern Rocky Mountain Science Center, Great Northern Landscape Conservation Cooperative and

Glacier National Park Conservancy. Samples were collected with permission under USGS permits to C.C.M. and J.J.G. S.H. was supported by NSF award DEB-0949532 (to D.W.W.) and S.J. and G.L. were funded in part by NSF award DOB-1639014. We thank Robin Bagley, Catherine Linnen, Schyler Nunziata and Tyler Tappenback for their assistance. We thank the University of Kentucky Center for Computational Sciences and Lipscomb High Performance Computing Cluster for providing computing resources. Lynn Hotaling, Peter Pearman and three anonymous reviewers provided valuable comments that improved the final version of the manuscript. Any use of trade, firm or product names is for descriptive purposes only and does not imply endorsement by the US Government.

DATA ACCESSIBILITY

All relevant associated data for this study, including complete RAD-seq loci information are available under the Data Dryad accession: https://doi.org/10.5061/dryad.4vg17.

ORCID

Scott Hotaling http://orcid.org/0000-0002-5965-0986

REFERENCES

Alexander, D. H., Novembre, J., & Lange, K. (2009). Fast model-based estimation of ancestry in unrelated individuals. *Genome Research*, *19*, 1655–1664.

Andrews, K. R., Good, J. M., Miller, M. R., Luikart, G., & Hohenlohe, P. A. (2016). Harnessing the power of RADseq for ecological and evolutionary genomics. *Nature Reviews Genetics*, *17*, 81–92.

Babron, M., Tayrac, D. E., Rutledge, D. N., Zeggini, E., & Génin, E. (2012). Rare and low frequency variant stratification in the UK population: Description and impact on association tests. *PLoS ONE*, *7*, e46519.

Baird, N. A., et al. (2008). Rapid SNP discovery and genetic mapping using sequenced RAD markers. *PLoS ONE*, *3*, e3376.

Baraer, M., Mark, B. G., McKenzie, J. M., Condom, T., Bury, J., Huh, K.-I., … Rathay, S. (2012). Glacier recession and water resources in Peru's Cordillera Blanca. *Journal of Glaciology*, *58*, 134–150.

Benestan, L., Gosselin, T., Perrier, C., Sainte-Marie, B., Rochette, R., & Bernatchez, L. (2015). RAD genotyping reveals fine-scale genetic structuring and provides powerful population assignment in a widely distributed marine species, the American lobster (*Homarus americanus*). *Molecular Ecology*, *24*, 3299–3315.

Brown, L. E., Hannah, D. M., & Milner, A. M. (2007). Vulnerability of alpine stream biodiversity to shrinking glaciers and snowpacks. *Global Change Biology*, *13*, 958–966.

Carrara, P. E. (1987). Holocene and latest Pleistocene glacial chronology, Glacier National Park, Montana. *Canadian Journal of Earth Sciences*, *24*, 387–395.

Catchen, J. M., Amores, A., Hohenlohe, P., Cresko, W., & Postlethwait, J. H. (2011). Stacks: Building and genotyping loci de novo from short-read sequences. *G3: Genes, Genomes, Genetics*, *1*, 171–182.

Catchen, J., Hohenlohe, P. A., Bassham, S., Amores, A., & Cresko, W. A. (2013). Stacks: An analysis tool set for population genomics. *Molecular Ecology*, *22*, 3124–3140.

Chattopadhyay, B., Garg, K. M., & Ramakrishnan, U. (2014). Effect of diversity and missing data on genetic assignment with RAD-Seq markers. *BMC Research Notes*, *7*, 841.

Excoffier, L., Dupanloup, I., Huerta-Sánchez, E., Sousa, V. C., & Foll, M. (2013). Robust demographic inference from genomic and SNP data. *PLoS Genetics*, *9*, e1003905.

Finn, D. S., & Adler, P. H. (2006). Population genetic structure of a rare high-elevation black fly, *Metacnephia coloradensis*, occupying Colorado lake outlet streams. *Freshwater Biology*, *51*, 2240–2251.

Finn, D. S., Encalada, A. C., & Hampel, H. (2016). Genetic isolation among mountains but not between stream types in a tropical high-altitude mayfly. *Freshwater Biology*, *61*, 702–714.

Finn, D. S., Khamis, K., & Milner, A. M. (2013). Loss of small glaciers will diminish beta diversity in Pyrenean streams at two levels of biological organization. *Global Ecology and Biogeography*, *22*, 40–51.

Foll, M., & Gaggiotti, O. (2008). A genome-scan method to identify selected loci appropriate for both dominant and codominant markers: A Bayesian perspective. *Genetics*, *180*, 977–993.

Garcia-Raventós, A., Viza, A., Tierno de Figueroa, J. M., Riera, J. L., & Múrria, C. (2017). Seasonality, species richness and poor dispersion mediate intraspecific trait variability in stonefly community responses along an elevational gradient. *Freshwater Biology*, *62*, 916–928.

Giersch, J. J., Hotaling, S., Kovach, R. P., Jones, L. A., & Muhlfeld, C. C. (2016). Climate-induced glacier and snow loss imperils alpine stream insects. *Global Change Biology*, *23*, 2577–2589.

Gutenkunst, R. N., Hernandez, R. D., Williamson, S. H., & Bustamante, C. D. (2009). Inferring the joint demographic history of multiple populations from multidimensional SNP frequency data. *PLoS Genetics*, *5*, e1000695.

Hall, M. H. P., & Fagre, D. B. (2003). Modeled climate-induced glacier change in Glacier National Park, 1850-2100. *BioScience*, *53*, 131–140.

Hansen, J., et al. (2005). Earth's energy imbalance: Confirmation and implications. *Science*, *308*, 1431–1435.

Hoffmann, A., Griffin, P., Dillon, S., Catullo, R., Rane, R., Byrne, M., … Joseph, L. (2015). A framework for incorporating evolutionary genomics into biodiversity conservation and management. *Climate Change Responses*, *2*, 1.

Hoffmann, A. A., & Sgrö, C. M. (2011). Climate change and evolutionary adaptation. *Nature*, *470*, 479–485.

Hotaling, S., Finn, D. S., Giersch, J. J., Weisrock, D. W., & Jacobsen, D. (2017). Climate change and alpine stream biology: Progress, challenges, and opportunities for the future. *Biological Reviews*, *92*, 2024–2045.

Hotaling, S., Hood, E., & Hamilton, T. L. (2017). Microbial ecology of mountain glacier ecosystems: Biodiversity, ecological connections, and implications of a warming climate. *Environmental Microbiology*, *19*, 2935–2948.

Jacobsen, D., Milner, A. M., Brown, L. E., & Dangles, O. (2012). Biodiversity under threat in glacier-fed river systems. *Nature Climate Change*, *2*, 361–364.

Janes, J. K., Miller, J. M., Dupuis, J. R., Malenfant, R. M., Gorrell, J. C., Cullingham, C. I., & Andrew, R. L. (2017). The K = 2 conundrum. *Molecular Ecology*, *26*, 3594–3602.

Jombart, T. (2008). adegenet: a R package for the multivariate analysis of genetic markers. *Bioinformatics*, *24*, 1403–1405.

Jombart, T., Devillard, S., & Balloux, F. (2010). Discriminant analysis of principal components: A new method for the analysis of genetically structured populations. *BMC Genetics*, *11*, 94.

Jordan, S., Giersch, J. J., Muhlfeld, C. C., Hotaling, S., Fanning, L., Tappenbeck, T. H., & Luikart, G. (2016). Loss of genetic diversity and increased subdivision in an endemic alpine stonefly threatened by climate change. *PLoS ONE*, *11*, e0157386.

Lischer, H., & Excoffier, L. (2012). PGDSpider: An automated data conversion tool for connecting population genetics and genomics programs. *Bioinformatics*, *28*, 298–299.

Macher, J. N., Rozenberg, A., Pauls, S. U., Tollrian, R., Wagner, R., & Leese, F. (2015). Assessing the phylogeographic history of the montane caddisfly *Thremma gallicum* using mitochondrial and restriction-site-associated DNA (RAD) markers. *Ecology and Evolution*, *5*, 648–662.

Meirmans, P. G. (2012). The trouble with isolation by distance. *Molecular Ecology*, *21*, 2839–2846.

Meirmans, P. G., & Van Tienderen, P. H. (2004). GENOTYPE and GENODIVE: Two programs for the analysis of genetic diversity of asexual organisms. *Molecular Ecology Notes*, *4*, 792–794.

Miller, M. R., Brunelli, J. P., Wheeler, P. A., Liu, S., Rexroad, C. E., Palti, Y., ... Thorgaard, G. H. (2012). A conserved haplotype controls parallel adaptation in geographically distant salmonid populations. *Molecular Ecology*, *21*, 237–249.

Miller, M. R., Dunham, J. P., Amores, A., Cresko, W. A., & Johnson, E. A. (2007). Rapid and cost-effective polymorphism identification and genotyping using restriction site associated DNA (RAD) markers. *Genome Research*, *21*, 240–248.

Milner, A. M., Brown, L. E., & Hannah, D. M. (2009). Hydroecological response of river systems to shrinking glaciers. *Hydrological Processes*, *23*, 62–77.

Monaghan, M. T., Spaak, P., Robinson, C. T., & Ward, J. V. (2001). Genetic differentiation of *Baetis alpinus* Pictet (Ephemeroptera: Baetidae) in fragmented alpine streams. *Heredity*, *86*, 395–403.

Muhlfeld, C. C., Giersch, J. J., Hauer, F. R., Pederson, G. T., Luikart, G., Peterson, D. P., ... Fagre, D. B. (2011). Climate change links fate of glaciers and an endemic alpine invertebrate. *Climatic Change*, *106*, 337–345.

Purcell, S., et al. (2007). PLINK: A tool set for whole-genome association and population-based linkage analyses. *The American Journal of Human Genetics*, *81*, 559–575.

Reusch, T. B. (2014). Climate change in the oceans: Evolutionary versus phenotypically plastic responses of marine animals and plants. *Evolutionary Applications*, *7*, 104–122.

Ricker, W. E. (1952) Systematic studies in Plecoptera. *Indiana University Publications Science Series*, 200 pp.

Sousa, V., & Hey, J. (2013). Understanding the origin of species with genome-scale data: Modeling gene flow. *Nature Reviews Genetics*, *14*, 404–414.

Treanor, H. B., Giersch, J. J., Kappenman, K. M., Muhlfeld, C. C., & Webb, M. A. H. (2013). Thermal tolerance of meltwater stonefly Lednia tumana nymphs from an alpine stream in Waterton-Glacier International Peace Park, Montana, USA. *Freshwater Science*, *32*, 597–605.

U.S. Fish and Wildlife Service. (2016). Endangered and threatened wildlife and plants; 12-month finding on a petition to list the western glacier stonefly as an endangered or threatened species; proposed threatened species status for Meltwater Lednian Stonefly and Western Glacier Stonefly. *Federal Register*, *81*, 68379–68397.

Wang, I. J., & Bradburd, G. S. (2014). Isolation by environment. *Molecular Ecology*, *23*, 5649–5662.

Ward, J. V. (1994). Ecology of alpine streams. *Freshwater Biology*, *32*, 277–294.

Wright, S. (1943). Isolation by distance. *Genetics*, *28*, 114.

BIOSKETCH

Scott Hotaling is a postdoctoral scholar in the School of Biological Sciences at Washington State University. His research is focused on leveraging genomic tools to better understand the adaptive potential of organisms in response to global change, particularly in alpine and polar ecosystems. Collectively, the authors form a collaborative research group interested in the links between population genetics, ecology and biodiversity in the face of glacier decline worldwide.

Author contributions: S.H., C.C.M., J.J.G, S.J., M.R.M., G.L. and D.W.W. conceived of the study. C.C.M., J.J.G., O.A.A. and M.R.M. collected the data. S.H. and D.W.W. performed the analyses. S.H. and D.W.W. wrote the manuscript. All authors read, contributed to and approved the final version.

SUPPORTING INFORMATION

Additional Supporting Information may be found online in the supporting information tab for this article.

How to cite this article: Hotaling S, Muhlfeld CC, Joseph Giersch J, et al. Demographic modelling reveals a history of divergence with gene flow for a glacially tied stonefly in a changing post-Pleistocene landscape. *J Biogeogr*. 2018;45:304–317. https://doi.org/10.1111/jbi.13125